Design Considerations for a Robotic Flying Fish

Amy Gao, Alexandra H. Techet
Department of Mechanical Engineering
Massachusetts Institute of Technology
Cambridge, Massachusetts 02139
{arg, ahtechet}@mit.edu

***Abstract*—This paper details an exploration into the design of an aerial-aquatic robotic vessel. A compact robot that could both swim underwater and glide in the air above water has many potential applications in ocean exploration and mapping, surveillance, and forecasting. In the first phase of this project, we focus on mechanical design concepts that would enable the biomimetic production of adequate thrust underwater. A brief review of precedent research concerning robotic fish and hydrodynamics is first presented, followed by an in-depth analysis of the mathematical theory relevant to the project. A passive model of a flying fish was constructed and launched from approximately 1 ft. underwater to determine the forces associated with overcoming drag underwater and exiting the water. Based on this, A number of conceptual designs which would produce the motion necessary for propulsion were formulated and are discussed from a mechanical design perspective. Various conventional and non-conventional actuators are reviewed, as well as a control scheme for the concepts presented. We end with a discussion of the future directions for this project, as well as the key challenges that remain to be addressed.**

Fig. 1. A flying fish gliding over the water surface. [1]

I. Introduction

In our vastly diverse and often hostile world, the creatures that survive are those that best adapt to their unique environments and dangers in them. Over millions of years, animals have evolved with a plethora of abilities sculpted to perfection over time. Flying fish exemplify the captivating precision with which animals have evolved. In the water, a multimodal sensor suite including a delicate array of neuromasts known as the lateral line allows them to instinctively sense and react to the changing flow of water around them to exploit drag-reducing and thrust-augmenting circumstances [1]. At the hint of a predator, powerful and intricately structured muscles contract rhythmically, generating enough thrust within an instant to propel the fish out of the water at speeds around 10 m/s. After water exit, the fish keeps the ventral lobe of its caudal fin submerged and flutters it at rates up to 35 Hz to reach a final take-off velocity of about 20 m/s [2]. Once aloft, oversized pectoral fins spread at once, and the fish glides for about 50 m. before dropping close to the water again. However, instead of just falling back into the water, the fish lowers its caudal fin below the water surface again and flutters it rapidly, exploiting the denser water near the surface for reactive force to produce enough thrust for another flight. Scientists have studied the behavior of flying fish for decades [3]–[6], and they speculate that this gliding ability of the flying fish has evolved as a means of escape from predators, but it yields the additional benefit of being a more efficient mode of transportation.

While flying fish have been studied in nature, and a number of biomimetic robots have been modeled after fish such as the tuna and the carp, no robot has been previously created with the ability to both swim in water and glide in the air above the water. However, the advantages to such a robot are evident. One of the prevailing characteristics of natural life is resourcefulness; flying fish use their full environment to survive (escape from predators) and thrive (travel with greater efficiency). The ocean is an enormous and vastly unexplored domain, and recent efforts have focused largely on comprehensive and integrated ocean mapping, surveillance of offshore platforms and structures, and ecological observing and forecasting. A compact robot that is capable of both swimming and flying could transform the areas of marine surveillance and ocean exploration.

In this paper, we consider the mechanical design challenges associated with biomimetic thrust production underwater. We begin with a brief history of research in the field, and a summary of relevant hydrodynamic theory. A key constraint in this project is the limited power density of modern actuators, so an estimate of the power density required to overcome the drag of swimming at 10 m/s is generated by Lighthill's elongated body theory. Additionally, an experiment was conducted to evaluate the hydrodynamic differences between mechanical and real fish, and how this affects the required

[1] Picture courtesy of Leif Nttestad, Institute of Marine Research, Norway.

0-933957-39-8 ©2011 MTS

power density. Subsequently, several actuation technologies are deliberated with regard to mechanical requirements and power density. Four conceptual designs based around the most promising actuators are then presented and their limitations discussed. Optimization of body flexion by genetic algorithms and implementation of a central pattern generator (CPG) is proposed for system control. We end with a summary of conclusions drawn from this exploration, and directions for further research.

II. Related Work

Research on robotic fish began in the mid 1900s due to a push for developing more efficient forms of underwater propulsion. Oscillating fin propulsion has high thrust efficiency and biomimetic underwater vehicles have the potential for being far more agile and maneuverable. They also minimize the possibility of accidents associated with propellers, such as ropes getting wound up or objects being sucked in.

Watanabe developed the first mechanical fish robot in 1976. It was 0.4 meters long and emulated a carp [7]. In 1980, researchers at the University of the Ryukyus made a 2.3 m long mechanical fish, which reached speeds of 1.5 m/s [7]. In 1995, Triantafyllou et. al. at MIT finished development of the first RoboTuna, a 1.3 m long biomimetic tuna. While its weight was supported by a strut hung from an electric train, it was able to reach speeds of 2.0 m/s, and research on it shed much light on Grays Paradox, as well as optimal oscillating frequencies [8].

Numerous additional robotic fish have been developed in recent years, including the MIT Robopike, the Coelacanthe, a robotic red snapper, the Essex Robotic Fish, and the Airacuda [9]–[12]. The majority of these strive towards increased biomimicry; some, such as the robotic red snapper, are nearly indistinguishable from actual fish. A few, such as the Airacuda, are demonstrations of the implementation of new technologies. None have been developed that swim as fast or efficiently as real fish. The fastest has been unable to exceed speeds of 2 body lengths per second (BL/s). In comparison, a velocity of 10 m/s is about 40 BL/s. [2]

III. Hydrodynamic Background

An understanding of the basic theory behind swimming is central to designing an underwater vehicle with comparable capabilities to fish. Breder distinguishes most fish as *anguilliform, ostraciiform* or *carangiform* swimmers based on the fraction of the body that is moved during steady swimming [5]. Fish with fusiform bodies, including the flying fish, comprise the carangiform class, which flex only the posterior half of their bodies as they swim. Carangiforms primarily generate thrust through creating propulsive waves of curvature and using the caudal fin as an oscillating foil. These methods of propulsion are well documented by past researchers [13]–[15], so they will only be summarized here. With the first technique, the fish contracts its muscles rythmically to create transverse waves of increasing amplitude, which push the surrounding water backward to create forward thrust, accelerating the fish quickly. Subsequently, while keeping the majority of the body rigid, the fish angles the caudal fin in an oscillatory manner, using it as a lifting surface and for vorticity control in order to swim with high efficiency. This project focuses on fast swimming as opposed to efficiency, so this section will be devoted to describing the energy associated with generating a propulsive wave.

For carangiform swimmers, the wavelength of the propulsive wave tends to be just longer than the body length and the amplitude of the wave tends to increase anteroposteriorly. For thrust to be generated, the phase velocity of the wave must be greater than the swimming speed [13]. The shape of the body approximates that of a wave with a growing envelope:

$$h(x,t) = a \cdot e^{-\gamma(x-L)} cos(k(x-L) - \omega t), \tag{1}$$

where h is the lateral motion, x the position along the body measured from the head, a is the trailing edge amplitude, L the body length, γ the rate of envelope increase, k the wave number of the propulsive wave, and ω is its frequency. This implies that for a robotic fish, at least two degrees of freedom are required to produce the half waveform in the posterior half of the body. The actuators and design must be capable of producing a traveling waveform of certain specifications, with enough force and speed to attain the necessary thrust.

IV. Thrust and Power Calculation

The minimal amount of thrust is that required to overcome the drag of swimming at the desired velocity of 10 m/s. An estimate of this drag force can be produced, given the dead-drag coefficient of a fish of similar size, $C_D \approx 0.02$ (at $Re = 2.54 \cdot 10^6$) [14]. The area used in this equation is the wetted area of a 0.25 m long flying fish, excluding the wings (which would be folded against the body during swimming).

$$\begin{aligned} F_D &= \frac{1}{2} C_D \rho U^2 A_w & (2)\\ &= 0.5 \cdot 0.02 \cdot 1000 \cdot 100 \cdot 0.023 & (3)\\ &= 23\ N & (4) \end{aligned}$$

Since the drag coefficient used here is determined from the dead drag of a rigid fish, this is a low estimate. Undulatory propulsion would result in higher pressure drag and friction drag [16]. For a mechanical fish, the drag force will also be much greater, as will be demonstrated later.

Given this estimate of the drag force experienced by a fish, the average power rate required to maintain a velocity of 10 m/s underwater can be produced using Lighthill's elongated body theory [17]. This theory is based on added mass effects, which produce a reactive force on the fish body when the fish swims using propulsive waves of the body. At high Reynolds number, much of the work done by the fish is used to push water out of the way, so this theory provides a good approximation. Strictly speaking, Lighthill's large amplitude elongated body theory would be more appropriate

[2]This value is calculated for a 0.25 m long fish, the average length of a flying fish. Hereafter, we assume that any fish or prototype referenced is of this length, and this velocity is the desired water exit velocity.

for carangiform motion, since it accounts for the additional yawing and sideslip of the head due to recoil forces [18]. However, the amplitude of tail motion we analyze here is an order of magnitude smaller than the body length, so the difference is not large. Therefore, to produce a rough power rate estimate here, we apply the small amplitude theory. By this, the time-average rate of work $\bar{P}$ is lateral velocity times rate of shedding of lateral momentum, or:

$$\bar{P} = [mU\overline{wW}]_{x=L}, \tag{5}$$

where U is the swimming velocity, L is the length of the fish (0.25 m), and m is the added mass. W is the lateral velocity of the fish (the time differential of the lateral position h), and w is the lateral velocity of the water at the fish surface. We are interested in the added mass at the trailing edge of the tail, and this can be calculated as:

$$m(x) = \frac{1}{4}\pi\rho s(x)^2 \tag{6}$$

$$m(L) = \frac{1}{4}\pi \cdot 1000 \cdot 0.115^2 \tag{7}$$

$$= 10.4\ kg/m, \tag{8}$$

where $s(x)$ is the span at position x. Given the approximate body shape of a carangiform swimmer (1), W and w at the trailing edge are:

$$W(L,t) = \frac{\delta h}{\delta t} = a\omega sin(-\omega t) \tag{9}$$

$$w(L,t) = \frac{\delta h}{\delta t} + U\frac{\delta h}{\delta x} \tag{10}$$

$$= a\omega\left(1 - \frac{U}{V}\right) sin(-\omega t) \tag{11}$$

$$-\gamma aUcos(-\omega t), \tag{12}$$

where V is the phase speed of the traveling wave formed by the body of the fish. This can be found by deriving an alternative expression for $\bar{P}$, which must also be equal to the sum of three terms: the rate at which the thrust produced performs work, the rate of kinetic energy increase of the surrounding water, and the energy flux into the wake. By setting this expression equal to (5), the time-average thrust force can be found as:

$$\bar{T} = [m(\overline{wW} - 0.5\bar{w}^2]_{x=L} \tag{13}$$

The minimal thrust force is that required to overcome the drag force, which was earlier determined to be on the order of 23 N. We solve these equations to find the phase speed of the propulsive wave, and subsequently the time-average power. For this, the following parameters were used: $a = 0.025$, $\gamma = 4$, $\omega = 220rad/s$, and $m(L) = 10.4$.

The required phase speed was found to be 12.18 m/s and the required time-average power was calculated as 281 W. For a 0.2 kg fish which is 50% muscle by weight, this relates to a muscle power density of 2810 W/kg.

For comparison, the muscles of biological fish are estimated to have specific power outputs of 20 W/kg and 80 W/kg for sustained and burst swimming, respectively [20]. However, these values were obtained for cold-water fish such as the trout, which have a maximum swimming speed of approximately 2 m/s. This is far lower than the 10 m/s that flying fish are able to reach. Since the required power scales roughly with U^2, it is reasonable that a muscle power density of 2810 W/kg would be required for a flying fish to swim at 10 m/s. The muscle power density of actual flying fish is unknown, but evidence would suggest that it is far greater than that of cold-water fish.

A mechanical fish will inevitably induce greater drag forces as a result of flow separation that occurs at sharp edges, and higher skin friction. To generate an estimate of the forces that would be experienced by a mechanical fish, a model of a flying fish was produced and launched from approximately 1 ft. underwater.

V. Mechanical Model Test

A passive flying fish model with spring-loaded wings was constructed by the fused deposition modeling (FDM) rapid prototyping technology. The coordinates for the main body are taken directly from the specimen *Exocoetidae parexoceoetioes*. The body was formed from acrylonitrile butadiene styrene (ABS) which was sealed by dissolving the top layer with acetone, and the pectoral fins (wings) are polyurethane coated nylon. A fiberglass beam provides support for each wing, and is mounted to the main body by two torsional springs with torques of 0.017 N-m. The model has a wingspan of 0.324 m, a pectoral fin area of 0.0252 m^2, and a ventral fin area of 0.0126 m^2. The body length is 0.25 m, the body volume is 145 cm^3, and its weight is approximately 145 g. A cavity in the center of the fish allows for the addition of weight to achieve neutral buoyancy in water. A 3d model of this design is shown in Fig. 2, and the constructed prototype is shown in Fig. 3.

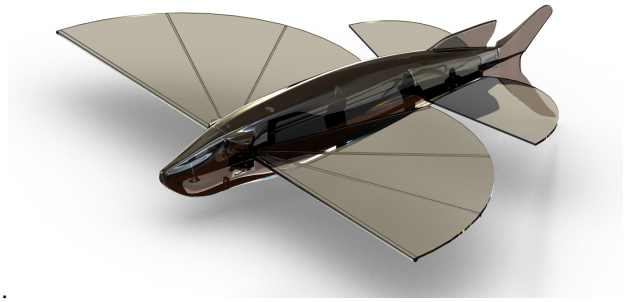

Fig. 2. CAD model of prototype flying fish, created in Solidworks.

A. Experiment Description

Experiments were conducted in the MIT Towing Tank, which is a 100 ft. long by approximately 10 ft. wide and 4 ft. deep tank of water. Two 5-ft lengths of latex tubing were used as a slingshot mechanism to launch the prototype from 1 ft. below the surface of the water. The tubing was attached to a metal strut approximately 5 ft. above the surface of the water on one end and a screw mounted on the bottom

Fig. 3. Constructed prototype of flying fish.

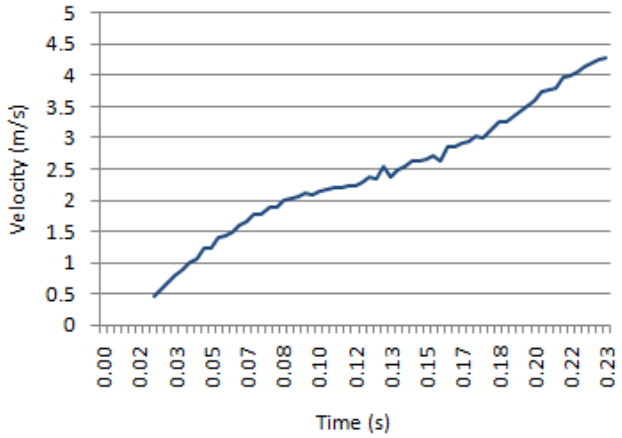

Fig. 4. Velocity of model as it is launched from below the water surface. Visible deformation of the free surface began to occur at 0.09 seconds, and the model breached the surface at 0.11 seconds.

of the prototype on the other end. 5 tests were performed, with the tubing stretched to 2 times its original length to pull the prototype out of the water. The wings were folded back initially, and allowed to extend naturally as the fish exited the water. A high speed camera was used to film the water exit scene, in order to measure the velocity at water exit. From this experiment, an estimate of the water drag force on the model could be produced.

B. Results

The model accelerated from rest to a water exit velocity of approximately 11.36 BL/s (2.84 m/s) in 0.147 seconds. The force exerted by the latex tubing is:

$$F = AY\frac{dL}{L} \quad (14)$$

$$= \pi(0.00318^2 - 0.00159^2)(2)(8.5 \cdot 10^5) \quad (15)$$

$$= 40\ N \quad (16)$$

A is the cross-sectional area of the tubing and Y is the Young's modulus of latex. Part of this force goes towards inertial acceleration:

$$F_A = (m + m_a)a \approx (2 \cdot 0.145) \cdot 19.3 = 5.6\ N \quad (17)$$

An additional 0.88 N counteracts gravity. The remaining 33.5 N of force is used to overcome drag forces, water exit forces, and other hydrodynamic forces. The power required to overcome these forces is about 95 W. As such, if half of the total mass of a 0.2 kg robotic fish were to be allocated for actuation, the actuators would need to have a specific power output of 950 W/kg. Since this is calculated for a water exit velocity of 2.84 m/s, even more power would be required at the desired water exit velocity of 10 m/s. Using Lighthill's elongated body theory to generate a power estimate at 10 m/s, we find that a specific power output of 4150 W/kg would be required.

VI. Water Exit Forces

Forces are also associated with exiting the water, and data from the experiments show that this force is not negligible (Fig. 4). As seen, forces during water exit visibly reduce the acceleration of the model from slightly before the nose of the fish reaches the surface and continue to have an effect on the model until it is well out of the water. The problem of water exit is nonlinear and unsteady, making it difficult to solve mathematically. However, numerical methods have been applied to investigate the dynamics of the problem successfully [21]–[23].

While the force required for water exit should not be neglected, it is not the critical factor in this design. Water exit is possible at speeds lower than the 10 m/s seen in nature, but at these lower speeds, the robot would be unable to generate adequate lift in the air to achieve sustained flights.

VII. Lift Force

To remain aloft, flying fish glide rather than actively flap their wings. As such, the lift produced must balance the weight of the fish for it to maintain a constant altitude. The lift coefficient has been found as approximately 0.8 for a 0.2 m long flying fish with 15 degree angle of attack [24]. Assuming a mechanical fish could be created with the same lift capabilities, the velocity of flight required to maintain a constant altitude is:

$$U = \left(\frac{W}{0.5 C_L \rho A}\right)^{\frac{1}{2}} \quad (18)$$

$$= \left(\frac{0.145 \cdot 9.8}{0.5 \cdot 0.8 \cdot 0.0252}\right)^{\frac{1}{2}} = 11.87\ m/s \quad (19)$$

At lower velocities, flights will be shorter, although still possible.

By analyzing the lift force, it is also possible to demonstrate the importance of keeping the vehicle small. If the fish were to be scaled up by just 2 times, the velocity of flight required to maintain a constant altitude would increase to 16.8 m/s. If it were to be scaled up to approximately 1 m in length, the velocity required would be 26.6 m/s. The thrust and power density it would take to reach these velocities underwater would be exponentially greater.

This shows that if an aerial-aquatic vehicle were to be developed, it should remain small and compact unless other forms of generating lift can be implemented.

VIII. Actuation

A key challenge in the design of a fast-swimming robotic fish is developing a compact and power-dense actuation system. As shown, a robotic flying fish may need to have actuators with a power density of 4150 W/kg or greater. It is important to consider this requirement when selecting appropriate actuators. Power to weight ratios of many actuators have been well documented [25], [26]. Characteristics such as ease of control, speed, stroke, and size are also important to take into consideration.

Traditional electromagnetic actuators such as DC motors and voice coils tend to be very large and heavy, with power densities on the order of 100 W/kg (but up to several kW/kg if high torque is not required and the motors are well cooled). Additionally, they are simple to integrate into systems and are available in a wide range of specifications.

Hydraulic actuators generally produce more force relative to their size and have power densities up to 10^4 W/kg, but would be limited by viscous effects at the high frequencies at which the device is likely to operate.

Pneumatic actuators and air muscles have power to weight ratios of up to 400 W/kg and inherent compliance which makes them compelling solutions for robotic actuation. However, their need for an air source and pump limits their application to robots that do not need to stay mobile over long distances or times.

Piezoelectric actuators are small and energy efficient with power densities up to 2000 W/kg, but their displacement tends to be on the order of micrometers, which is far too small for most robotic applications.

Shape memory alloys (SMA) have shown much promise in emerging robotic technologies due to their minimal size, moderate force to weight ratio (100 W/kg) and corrosion resistance. However, they generally operate at lower frequencies and consume vast amounts of power, particularly when submersed in water.

Electroactive polymers (EAP) have also been successful in recent robotic developments, but can be difficult to model and generally lack the speed and force potential to produce quick, powerful strokes.

Given the limitations of most non-conventional actuation technologies, traditional electromagnetic actuators appear to be the most promising option. Numerous conceptual designs were formulated around these actuators, and four were selected to be discussed in the following section. These concepts utilize novel ideas in mechanical design which show promise for biomimetic propulsion.

IX. Conceptual Designs

Conceptual designs were formulated around the design requirement of creating a propulsive wave of curvature, using traditional electromagnetic actuators.

A. Linkage System With Helical Driveshaft

The first concept is a low mechanical impedance linkage design which is driven by a helical driveshaft. Parallel sections of the part of the tail that is to be driven are connected through linkages that pivot on the dorsoventral plane, such that each section has only one degree of freedom with respect to each neighboring plane. This system is illustrated in Fig. 5.

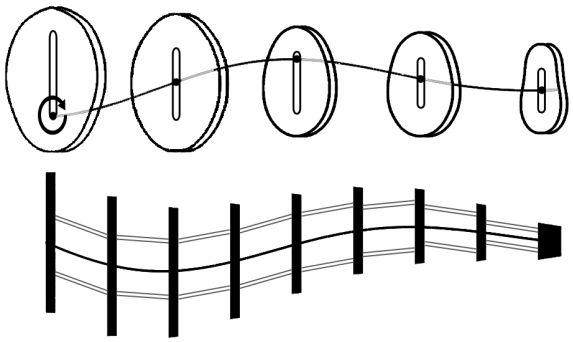

Fig. 5. Sketch of linkage system with a helical driveshaft. Upper: cross-sectional side view of every other plane. Lower: top view of generated curvature. As the driveshaft is rotated at the base of the tail, it is allowed to slide dorsoventrally along each section while creating movement of each section from side to side.

One actuator is sufficient to drive this design, and since only unidirectional rotary motion is required of the actuator, the conventional DC motor was selected. The motor is attached to the helical driveshaft at the base of the tail, and as the shaft turns, the helical driveshaft will also rotate. The shape of the helix dictates the radius of motion at each plane. Since the cross-sectional height of the body decreases toward the tip of the tail, the radius of the helix must decrease accordingly to stay within the constraints of the body. Dorsoventral slots in each section of the fish, as depicted in Fig. 5, will harness the sway motion of the helix while leaving the heave motion unconstrained. Therefore, as the helix turns, each section of the fish will be forced to move from side to side. The linkages prevent each section from heaving with the helix, and the sinusoidal shape of the helix governs the shape and length of the wave on the body. In the example shown, one full wavelength occupies the body; however, this can be readily changed to account for optimal parameters.

Due to the linkages, as the design is actuated each section of the fish will surge forward and backward slightly as well as sway from side to side. This imitates the biological figure-of-eight motion that is produced by each point along the body of a real fish. It is this figure-of-eight motion that results in constant forward propulsion, and by mimicking it, this design will be capable of doing the same. As the motor is driven in one direction, forward thrust will be produced, and negative thrust would be produced if the motor were to be driven in the other direction.

The strength of this design is in its simplicity. While most existent designs require reciprocating motion of its actuators,

the unidirectional operation of the motor in this concept eliminates the need for complex electronics or control schemes, and allows for the actuator to be used to its full potential.

A possible barrier to the success of this design exists in the fact that the amplitude of the wave produced by the body decreases anteroposteriorly. Lighthill's theory suggests that the average thrust force produced increases directly with the added mass at the trailing edge, which increases with the amplitude of motion at the tip of the tail (see Eqn. 13). Additionally, it is evident that for carangiform swimmers, the traveling wave increases in amplitude toward the rear of the body. It is unclear whether high thrust forces can be produced in the opposing case, and further development of this concept would be required to resolve this issue.

B. Fin Ray Design Driven by Voice Coils

The Fin Ray Effect is a biomechanical principle inspired by fish fins which translates linear motion into bending motion. It has been integrated into and shown to produce thrust in robotic fish, rays, and jellyfish [27]. A basic sketch of how this principle works is shown in Fig. 6.

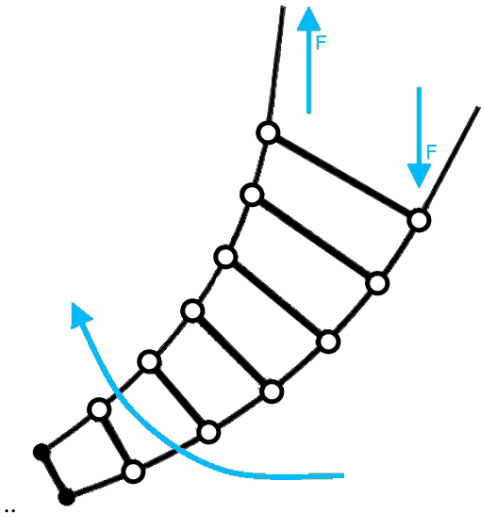

Fig. 6. Sketch of kinematic principle of the Fin Ray Effect.

A system employing the Fin Ray Effect is created by joining the ends of two flexible beams, and optionally using rigid bars to space apart the beams at regular intervals. Then, by applying longitudinal force to the base of the two beams, the structure can be made to curve, and to simulate traveling waves. A similar mechanism is the zipper in a Ziploc bag. By forcing the two sides to slide against each other on one end, a curve can be made to form along the entire length of the zipper. By actuating the two sides in a rhythmic manner, a traveling wave can be created.

By integrating the Fin Ray Effect into a robotic fish, propulsive waves of curvature may be formed with a low number of actuators at the base of the tail. Here, we have selected voice coils because of the simplicity of control and the smooth, fast linear motion produced.

This design may be restricted by the high mechanical impedance of moving in water. If the higher drag forces in water dampen the wave too strongly, a traveling wave of increasing amplitude may not be able to be produced. Given Lighthill's theory, if the trailing edge amplitude is small, forward thrust may not be generated.

C. Servomotor Crossover Tendon Configuration

The third design is developed around the concept of crossover tendons. The crossed tendon drive is a novel mechanism that uses actuated tendons to articulate serpentine robots. Unlike traditional tendon drives, the tendons in this design are crossed at intervals along the length of the body so as to travel through channels of varied circumferential angle [28]. As a result of this, each tendon produces a nonlinear distribution of bending torque, and by combining multiple such distributions, a range of smooth sinusoidal shapes can be achieved. The advantage of a crossed tendon drive over a traditional tendon drive is that the number of actuators required to yield complex bending motions is greatly reduced. Therefore, with only three actuators, a range of motions could be produced and optimized for forward thrust. A diagram of the crossed tendon drive integrated into a fish robot is depicted in Fig. 7.

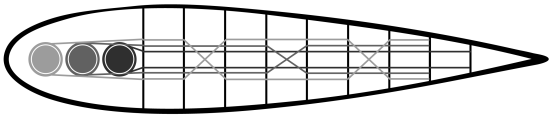

Fig. 7. Diagram of crossover tendon configuration actuated by servomotors (top view).

In this design, rigid sections at regular intervals along the length of the robot are connected by a flexible spine. Three pairs of antagonistic tendons run through channels in each section. The innermost pair does not contain any crossings; the second pair contains one, and the third pair contains two. A greater number of crossings in an area results in finer control of that area, and crossings which exist on the same tendon pair are actuated in a coupled manner. For instance, in the arrangement of Fig. 7, actuating the second tendon pair will result in greater bending in the middle of the tail, while actuating the third pair will result in simultaneous bending at the front and back of the tail. Actuating the first pair will result in uniform bending. The arrangement of crossovers and the radial distance between the spine and the tendons determine the relationship between tendon actuation and bending of the body. Each tendon pair is actuated by a servomotor, which has the advantage of simple position control.

Due to the nonlinear nature of the crossed tendon drive, the system is difficult to model and control. However, there are multiple ways of addressing this challenge, and additional research into this concept could realize a solution.

D. Traditional Joint Actuation

Finally, a traditional and well tested design is that of multiple rigid sections which are linked and actuated at joints by servomotors or DC motors [8], [9], [29]. The benefit to such an approach is the ability to control each degree of freedom precisely and therefore create any body shape easily. However, previous robotic fish of this design have not succeeded in achieving the velocities we hope to achieve here. Therefore, while the design is well attested to, it may not be the best approach.

X. System Control

For designs (b) - (d), a control algorithm would be necessary to modulate the motion of the multiple actuators in a way that will result in a thrust-generating body motion. Developing this algorithm using machine learning concepts would be optimal, as it would allow for continual adaptation, as well as some human error in the application of the relevant hydrodynamic theory. Numerous control strategies have been evaluated and implemented on serpentine-type robots in the past [29], [30], and there are many possible approaches that could be taken for these designs. One approach is to use a central pattern generator (CPG).

A CPG is a neural network that generates rhythmic patterns of muscle activation such as breathing and walking, and swimming for fish. By activating the array of muscles in a rhythmic sequence, a fish is able to decompose the high-dimensional intricate act of swimming into something basic and adaptable. This concept is easily extendable to robotics, and several researchers have already implemented CPGs in swimming robots. The CPG models used in swimming robots are typically inspired by that of the natural lamprey, and have been implemented using finite-state machines [31], cellular networks [32] and systems of coupled oscillators [33].

CPGs must be trained, but there are numerous ways to do this as well. For instance, a genetic algorithm could be used to evolutionarily create an optimal pattern of flexion, as demonstrated by Barrett et. al. [8].

XI. Conclusions and Future Directions

Through this design exercise, several important conclusions have been reached that are definitive to the possibility of successfully building a flying fish robot in the future.

1) The development of an autonomous flying fish robot capable of reaching velocities of 10 m/s underwater may not be possible without advancements in actuation technologies. The required specific power output of over 4000 W/kg is far greater than the specific power output of conventional electromagnetic actuators, which is on the order of 100 W/kg. However, under certain conditions, a power output of several kW/kg could be reached, and the conditions under which this is possible should be further explored.
2) By scaling the vehicle up in size, it would be possible to reduce the power density required and allow for the integration of actuators of higher power density, since this increases with actuator size. However, a size increase would also increase the velocity that must be attained for extended gliding flight. A balance between these tradeoffs must be achieved for optimal performance.
3) Since the required power density scales roughly with U^2, reducing the desired swimming velocity drastically reduces the power density requirement. For instance, by reducing the desired velocity to 5 m/s, a power density of only 462 W/kg would be required, which is far more achievable. Therefore, future work could focus on the development of a flying fish that swims more slowly and therefore has slightly compromised gliding ability, or one that is able to continue to accelerate by other means after exiting the water.
4) In thrust generation by a propulsive wave of curvature, the average thrust produced appears to be directly related to the trailing edge amplitude. As a result, it may be impossible or inefficient to generate thrust with a traveling wave of decreasing amplitude. Further tests may be performed to resolve this.
5) If this is true, concept A would not work, and concept B also may not work if the high mechanical impedance of water prevented the wave from propagating throughout the tail. Since the direction of wave propagation opposes the direction of wave amplitude decrease, the wave motion must be created superficially. There would be no way to create a propagating wave, only a precisely actuated body in the shape of a wave.

In summary, more testing should be performed to determine the feasibility of developing a flying fish robot. Regardless of this, however, much inspiration can be taken from flying fish in nature for the advancement of some modern technologies. For instance, in recent years much research has focused on development of the ground effect vehicle (GEV), which operates much like the flying fish [34]. GEV's take advantage of a cushion of high pressure air generated between them and the water for higher efficiency flight, when flying within approximately a wingspan of the water. This concept holds much promise due to the greatly increased lift and reduced drag in ground effect flight, but there are still many issues to be addressed regarding control and stability to disturbances in the form of high waves or wind gusts which are more prevalent in the zone of flight. Insight from flying fish may address some of these problems. The extension of a fin from the vehicle to the water, for instance, could provide greater controllability, as well as a more efficient method of propulsion. The ability of flying fish to taxi across the surface of the water utilizes the denser water for reactive force to travel through the less dense air. While this project has demonstrated the difficulty of reaching the desired water exit velocity of 10 m/s underwater, it may be possible to exit the water at a lower velocity and continue to accelerate by this principle once in the air. Future work may include development of control schemes for stabilizing a gliding vehicle with a submerged oscillating foil above the surface of the water.

ACKNOWLEDGMENT

This material is based upon work supported by the National Science Foundation Graduate Research Fellowship under Grant No. 0645960. Thanks also to Ben Johnson for stimulating discussions and his help with the experiments in this project!

REFERENCES

[1] H. Bleckman, *Reception of Hydrodynamic Stimuli in Aquatic and Semiaquatic Animals*. Stuttgart, Germany: Fischer-Verlag, 1994.
[2] H. Hertel, *Structure, Form and Movement*. New York: Reinhold, 1966.
[3] G. W. Baird, The Flight of the Flying-Fish, *Science*, vol. 8, no. 178, pp. 10-12, 1886.
[4] W. B. Barrows, Flight of the Flying-Fish. *Science*, vol. 1, no. 21, p. 603, 1883.
[5] C. M. Breder, On the Structural Specialization of Flying Fishes from the Standpoint of Aerodynamics. *Copeia*, vol. 1930, no. 4, pp. 114-121, 1930.
[6] F. E. Fish, Wing Design and Scaling of Flying Fish With Regard to Flight Performance. *Journal of Zoology*, vol. 221, pp. 391-403, 1990.
[7] M. Nagai, *Thinking Fluid Dynamics with Dolphins*. Tokyo, Japan: Ohmsha, Ltd, 2002.
[8] D. Barrett, M. Grosenbaugh, and M. Triantafyllou. The Optimal Control of a Flexible Hull Robotic Undersea Vehicle Propelled by an Oscillating Foil, in *Proc. 1996 Symposium on Autonomous Underwater Vehicle Technology*, Monterrey, CA, Jun. 1996, pp. 1-9.
[9] Robotic-fish.net. [Online].
Available: http://robotic-fish.net/index.php?lang=en&id=robots
[10] J. Conte, Y. Modarres-Sadeghi, M. N. Watts, F. S. Hover, and M. S. Triantafyllou, A Fast-Starting Mechanical Fish that Accelerates at 40 ms^{-2}, *Bioinspiration and Biomimetics*, vol. 5, no. 3, pp. 1-9, 2010.
[11] H. Hu, Biologically inspired design of autonomous robotic fish at Essex, in *IEEE SMC UK-RI Chapter Conference, on Advances in Cybernetic Systems*, pp. 38, 2006.
[12] W. Stoll *et al.* (2006) Airacuda. [Online]
Available: http://www.festo.com/cms/en_corp/9761.htm
[13] J. J. Videler, *Fish Swimming*. London, England: Chapman & Hall, 1993.
[14] R. W. Blake, *Fish Locomotion*. Cambridge, U.K.: Cambridge University Press, 1983.
[15] P. W. Webb, "Form and function in fish swimming," *Scientific American*, vol. 251, pp. 58-68, 1984.
[16] W. H. Allen, "Underwater flow visualization techniques," *NOTS Technical Publication*, China Lake, CA: US Naval Ordinance Test Station.
[17] M. J. Lighthill, "Aquatic Animal Propulsion of High Hydromechanical Efficiency," *Journal of Fluid Mechanics*, vol. 44, no. 2, pp. 265-301, 1970.
[18] M. J. Lighthill, "Note on the Swimming of Slender Fish," *Journal of Fluid Mechanics*, vol. 9, pp. 305-317, 1960.
[19] P. Legac, F. Fish, T. Williams, and T. Wei, "DPIV Measurements on Dolphins: Examining Gray's Paradox," in *APS Division of Fluid Dynamics Meeting Abstracts*, Nov. 2007.
[20] R. Bainbridge, "Problems of Fish Locomotion," *Symposia of the Zoological Society of London*, no. 5, pp. 13-32, 1961.
[21] Q. Ye, and Y. He, "Double-Parameter Perturbation Solution to 3-D Nonlinear Problem of Oblique Water Exit," *Journal of Hydrodynamics*, vol. 4, pp. 96-103, 1991.
[22] J. P. Moran and K. P. Kerney, "On the Small-Perturbation Theory of Water-Exit and Entry," in *Developments in Mechanics*, vol. 2, Pergamon, Oxford, 1963.
[23] D. G. Dommermuth, and D. K. P. Yue, "Numerical Simulations of Nonlinear Axisymmetric Flows with a Free Surface", *J. Fluid Mech.*, vol. 178, pp. 195-219, 1987.
[24] H. Park and H. Choi, Investigation of Aerodynamic Capabilities of Flying Fish in Gliding Flight, *IUTAM Symposium on Unsteady Separated Flows and Their Control*, vol. 14, pp. 27-33, 2009.
[25] H. Mochizuki, H. Mekaru, S. Kusumi, N. Sato, M. Shimizu, M. Yamashita, O. Shimada, and T. Hattori, "Design of Solenoidal Electromagnetic Microactuator Utilizing 3D X-ray Lithography and Metallization," *Microsyst Technol*, vol. 13, pp. 547550, 2007.
[26] K. Ikuta, "Micro/Miniature Shape Memory Alloy Actuator," in *Proc. IEEE Int. Conf. Robotics and Automation*, Cincinnati, OH, May 1990, pp. 2156-2161.
[27] Fin Ray Effect. [Online]
Available: http://www.festo.com/cms/nl-be_be/16394.htm
[28] A. Trazkovich, M. Taylor, and G. Pratt. "Crossed-Tendon Drive: An Economic Mechanism for Articulating Endoscopes and Serpentine Robots," *The International Journal of Robotics Research*, submitted for publication.
[29] J. Yu, S. Wang, and M. Tan, "Basic Motion Control of a Free-Swimming Biomimetic Robot Fish," in *Proc. IEEE Conf. Decision and Control*, Maui, HI, Dec. 2003, pp. 1268-1273.
[30] D. Zhang, D. Hu, L. Shen, and H. Xie, "A Bionic Neural Network for Fish-Robot Locomotion," *Journal of Bionic Engineering*, vol. 3, pp. 187-194, 2006.
[31] C. Wilbur, W. Vorus, Y. Cao, and S. N. Currie, "A Lamprey-Based Undulatory Vehicle," *Neurotechnology for Biomimetic Robots*. J. Ayers, J. L. Davis, and A. Rudolph, Eds. Cambridge, MA: Bradford/MIT Press, 2002.
[32] P. Arena, "A Mechatronic Lamprey Controlled by Analog Circuits," in *Proc. IEEE Mediterannean Conference on Control and Automation*, Dubrovnik, Croatia, Jun. 2001.
[33] A. J. Ijspeert, and A. Crespi, "Online Trajectory Generation in an Amphibious Snake Robot Using a Lamprey-Like Central Pattern Generator Model," in *Proc. IEEE international Conference on Robotics and Automation*, Roma, Italy, Apr. 2007, pp. 262-268.
[34] E. Cui, "Surface Effect Aero-Hydrodynamics and its Applications," *Sādhanā*, vol. 23, no. 5-6, pp. 569-577, 1998.